Journal of Materials Chemistry b815401e

PAPER

1

Urea assisted hydroxyapatite mineralization on MWCNT/CHI scaffolds

María J. Hortigüela, María C. Gutiérrez,* Inmaculada Aranaz, Matías Jobbágy, Ander Abarrategi, Carolina Moreno-Vicente, Ana Civantos, Viviana Ramos, José L. López-Lacomba, María L. Ferrer and Francisco del Monte*

We describe the mineralization of *ca.* 1 μm flower like hydroxyapatite crystals on the internal macroporous surface of MWCNT/CHI scaffolds.

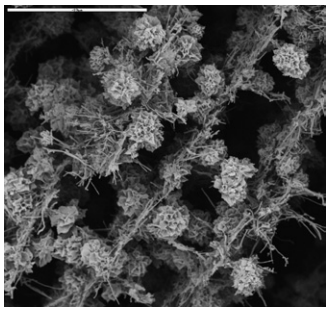

Please check this proof carefully. **Our staff will not read it in detail after you have returned it**.

Translation errors between word-processor files and typesetting systems can occur so the whole proof needs to be read. Please pay particular attention to: tabulated material; equations; numerical data; figures and graphics; and references. If you have not already indicated the corresponding author(s) please mark their name(s) with an asterisk. Please e-mail a list of corrections or the PDF with electronic notes attached – do not change the text within the PDF file or send a revised manuscript.

Please bear in mind that minor layout improvements, e.g. in line breaking, table widths and graphic placement, are routinely applied to the final version.

We will publish articles on the web as soon as possible after receiving your corrections; no late corrections will be made.

Please return your **final** corrections, where possible within **48 hours** of receipt by e-mail to: proofs@rsc.org

Reprints—Electronic (PDF) reprints will be provided free of charge to the corresponding author. Enquiries about purchasing paper reprints should be addressed via: http://www.rsc.org/Publishing/ReSourCe/PaperReprints/. Costs for reprints are below:

Reprint costs

No of pages	Cost for 50 copies	Cost for each additional 50 copies
2–4	£190	£120
5–8	£315	£230
9–20	£630	£500
21–40	£1155	£915
>40	£1785	£1525

Cost for including cover of journal issue:
£55 per 50 copies

Urea assisted hydroxyapatite mineralization on MWCNT/CHI scaffolds

María J. Hortigüela,[a] María C. Gutiérrez,*[a] Inmaculada Aranaz,[a] Matías Jobbágy,[a] Ander Abarrategi,[bc] Carolina Moreno-Vicente,[b] Ana Civantos,[b] Viviana Ramos,[c] José L. López-Lacomba,[b] María L. Ferrer[a] and Francisco del Monte*[a]

Received 3rd September 2008, Accepted 2nd October 2008
First published as an Advance Article on the web ?????
DOI: 10.1039/b815401e

Urea assisted hydroxyapatite (HAp) mineralization was performed on scaffolds composed of a major fraction of multiwall carbon nanotubes (MWCNT, 85 wt.%) and a minor one of chitosan (CHI, 15 wt.%). The MWCNT/CHI scaffolds were synthesized through a cryogenic process (so called ISISA, ice segregation induced self-assembly) that allowed the achievement of macroporous monoliths whose structure resembled a chamber-like architecture in the form of interconnected MWCNT/CHI sheets arranged in parallel layers crossed by pillars. The mineralized architectures were composed of flower like hydroxyapatite (HAp) crystalline clusters of *ca.* 1 μm, homogeneously distributed throughout the internal surface of the scaffold macrostructure. HAp mineralized MWCNT/CHI scaffolds were characterized by X-ray diffraction (XRD), infrared spectroscopy (FTIR) and scanning and transmission electron microscopy (SEM and TEM, respectively). Calibrated energy dispersion X-ray spectroscopy (EDS) and selected-area electron diffraction (SAED) were also performed in the transmission electron microscope to further HAp characterization. Preliminary *in vitro* experiments demonstrated the suitability of HAp mineralized MWCNT/CHI scaffolds for bone tissue growth.

Introduction

The huge demand for tissue engineering scaffolds has recently promoted substantial efforts toward biomimetic mineralization in hydrogel matrices, both natural and synthetic ones. The nucleation process seems to be initiated at the organic–inorganic interface, the organic component providing a nucleating matrix for the inorganic mineral.[1,2,3] In natural processes, the mineral-binding proteins are responsible for the modulation of the mineralization process by either preventing nucleation through the complexation of ions in solution or stabilizing precursor particles and preventing particle agglomeration by surface binding. In synthetic processes (hence, in the absence of proteins), bone like properties have also been engendered successfully. In both cases, the dissolution of calcium phosphate precursor and subsequent re-crystallization is the general trend followed by complete mineralization and, eventually, by bone tissue formation.[4,5]

There is quite a list of self-assembled organic superstructures forming 3D architectures to template inorganic materials with controlled morphologies. Most of these scaffolds have organic nature (*e.g.*, supramolecular gels,[6] natural polymers like gelatin,[7] collagen[8] or chitosan (CHI),[9] polymer blends like poly (α-hydroxyester) and poly(lactide-*co*-glycolide),[10] hydrophilic block copolymers,[11,12] polymer hydrogels like PHEMA and derivates,[13] polyaspartates,[14] or linear aspartic acid rich peptides,[15] among others) but some others may also have inorganic/ceramic nature (*e.g.*, opals of $CaO\text{-}SiO_2$[16]). Less usual is the use of carbon nanotubes (CNT) as substrates for mineralization purposes, with just a couple of works growing hydroxyapatite (HAp) on single-wall and multi-wall carbon nanotube (SWCNT and MWCNT, respectively) films,[17,18] but none (to our knowledge) on CNT scaffolds.

We have recently reported on the preparation of MWCNT/CHI scaffolds through a cryogenic process (so called ISISA, ice segregation induced self-assembly).[19] ISISA is a simple and versatile bottom-up process, based on the unidirectional immersion of a colloidal aqueous suspension into a liquid nitrogen bath. The process has demonstrated its suitability for the preparation of inorganic, organic and hybrid macroporous monoliths and fibers by freeze-drying different hydrogels and aqueous colloidal suspensions.[20] Moreover, the process is highly biocompatible (*i.e.* it begins from an aqueous suspension and runs in the absence of further chemical reactions, avoiding potential complications associated with by-products or purification procedures) so that we have been able to immobilize proteins, liposomes (*e.g.*, membrane structures that mimics that of cells) and even bacteria within the resulting scaffolds.[19b,21] Moreover, we have recently demonstrated the suitability of MWCNT/CHI scaffolds for tissue engineering purposes, in particular, for the ectopic formation of bone tissue in muscle tissue after implantation of the scaffold with rhBMP-2 (a potent osseoinductor protein that promotes the differentiation of non-differentiated cells towards osteoblastic lineage) adsorbed on its macrostructure.[19c] Besides collagen expressing cells, the

[a]*Instituto de Ciencia de Materiales de Madrid-ICMM, Consejo Superior de Investigaciones Científicas-CSIC, Campus de Cantoblanco, 28049, Madrid, Spain. E-mail: mcgutierrez@icmm.csic.es; delmonte@icmm.csic.es; Fax: +34 91 3720623; Tel: +34 91 3349000*
[b]*Instituto de Estudios Biofuncionales, Universidad Complutense de Madrid, Paseo Juan XXIII 1, 28040, Madrid, Spain*
[c]*Noricum Inc, Departamento de I + D, Parque Científico de Madrid, C/ Santiago Grisolía 2, Tres Cantos, 28760, Madrid, Spain*

incorporation of HAp precursors would also be of help for bone tissue regeneration. Thus, the preparation of mineralized MWCNT/CHI scaffolds also containing HAp precursors and/or crystals is of interest to complement our previous work with rhBMP-2.

In this work, mineralization of MWCNT/CHI scaffolds with HAp crystals was performed through a urea assisted process.[22,23,24] Thermal treatment of urea aqueous solutions at 90 °C promotes urea decomposition into carbon dioxide and ammonia as main by-products. Ammonia release causes a gradual pH rise that, for aqueous solutions also containing calcium and phosphate salts (in stoichiometric ratio), results in HAp crystals precipitation. In the presence of MWCNT/CHI scaffolds (*i.e.* for scaffolds soaked in the urea aqueous solution), the resulting HAp crystals precipitated on the internal surface of the scaffold macrostructure. The experimental conditions required for homogeneous or heterogeneous distribution of HAp crystals throughout the internal MWCNT/CHI macrostructure were studied. The resulting HAp mineralized MWCNT/CHI scaffolds were characterized by FTIR, XRD, SEM, EDX, TEM and electron diffraction. Preliminary *in vitro* experiments demonstrated the suitability of HAp mineralized MWCNT/CHI scaffolds for viability and proliferation of preosteoblastic C2C12 cells which, in the presence of the recombinant human protein BMP-2 (rhBMP-2), could even differentiate towards collagen expressing cells.

Experimental

Materials

Chitosan (CHI, Batch #04607JB, Av. Mol. Wt. 440 KDa), HAp (reagent grade, powder), urea (reagent grade, 98%), glutaraldehyde (GA, 50 wt.% in water) and MWCNT (diameter 110–170 nm, length 5–9 μm) were purchased from Sigma-Aldrich. Water was distilled and deionized.

Preparation of MWCNT-CHI buffered suspensions

CHI solutions (1 wt.%) were prepared by dissolving CHI flakes (0.5 g) in 50 mL of an aqueous solution of acetic acid (0.05 M, pH 5.5). MWCNTs were functionalized by refluxing 500 mg of MWCNTs in 25 mL of nitric acid (14 M) at 130 °C for 6 hours. The resulting functionalized MWCNTs were repeatedly washed with distilled water until complete nitric acid removal, and left to dry. Functionalized MWCNTs (90 mg) were sonicated and vigorously stirred in 1.5 mL of CHI solution (1 wt.%) to obtain a homogeneous dispersion.

ISISA processing for MWCNT/CHI scaffolds preparation

The suspensions (1 mL) were collected in insulin syringes and dipped (at 5.9 mm/min) into a cold bath maintained at a constant temperature of −196 °C. The unidirectionally frozen samples were freeze-dried using a ThermoSavant Micromodulyo freeze-drier. The resulting monoliths kept both the shape and the size of the insulin syringes (in this particular case) and of any container where the suspensions might be collected prior to freezing.

Urea assisted mineralization of MWCNT/CHI scaffolds

Prior to mineralization, MWCNT/CHI scaffolds were exposed (at room temperature and for 24 hours) to GA vapors for CHI cross-linking and structure reinforcement. After GA vapor exposure, the MWCNT/CHI scaffolds were aerated for a further 24 hours. Two slightly different procedures were followed for mineralization. Procedure (a) was based on the under-vacuum soaking of a monolithic portion of MWCNT/CHI scaffold in 5 mL of an acidic aqueous solution of HAp (15 mg/mL, pH 2.5) containing urea (2 M). The solution was heat treated at 90 °C for different times (4, 8 and 12 hours). Procedure (b) was also based on the under-vacuum soaking of a monolithic portion of MWCNT/CHI scaffold in 5 mL of an acidic aqueous solution of HAp (15 mg/mL, pH 2.5) containing urea (2 M). However, the soaked MWCNT/CHI scaffold was taken out of the HAp solution after 40 minutes, and heat treated at 90 °C for 4 and 12 hours.

Sample characterization

The morphology of MWCNT/CHI scaffolds was investigated using a Zeiss DSM-950 scanning electron microscope. The morphology of HAp crystals was investigated by a 200-KeV JEOL JEM-2000FX electron transmission microscope (TEM), while the selected area electron diffraction (SAED) was used to show the crystallinity of the sample, and calibrated energy dispersion X-ray spectroscopy (EDS) was used to identify the Ca/P ratio of a selected area of the sample. Fourier transform infrared spectra (FTIR) were recorded in a NICOLET 20 SXC FTIR. XRD patterns were obtained in a Bruker D8 Advance diffractometer using CuKα radiation (step size, 0.05°; counting time, 3.5 sec). The chemical analyses were performed by inductively coupled plasma atomic emission spectrometry (ICP-AES), using a Thermo Jarrell Ash model Iris Advantage spectrophotometer.

In vitro cell culture assays

The *in vitro* assays with MWCNT/CHI scaffolds were conducted on monoliths with cylindrical shape (dimensions: 7 mm diameter and 2 mm thickness). Monoliths were exposed to overnight UV light irradiation for sterilization. Every monolith was placed into a 24-well cell culture plate well (16 mm diameter, from Corning Incorporated Costar). C2C12 cells (muscle myoblast, mouse, ATCC CRL 1772, Manassas, Virginia) were seeded onto scaffolds (2×10^5 cells per scaffold). The seeded scaffolds were cultured in DMEM medium also containing 10% fetal bovine serum and antibiotics (100 U/ml penicillin and 100 μg/ml streptomycin sulfate) and studied after 4 days of culture by environmental scanning electron microscopy (ESEM) using a Phillips XL30ESEM microscope. 3-(4,5-Dimethylthiazol-2-yl)-2,5-diphenyltetrazoliumbromide (MTT) *in vitro* toxicology and cell proliferation assays were performed (on both the MWCNT/CHI scaffolds and the culture medium at the plate well eventually squeezed from the scaffolds) by adding reconstituted MTT (a 1/10 dilution; 40 μL MTT in 400 μL medium) to the cell culture medium. After incubation for 2.5 h, 440 μL of MTT solubilization solution were added and the absorbance at 570 nm was measured in a Microplate Reader (Biotek FL-600). The absorbance at 690 nm was also measured as background.

ART ■ B815401E

Cell differentiation on MWCNT/CHI scaffolds

C2C12 cell differentiation was induced by using a recombinant human bone morphogenetic protein-2 (rhBMP-2, from Noricum Inc.). rhBMP-2 was obtained through genetic engineering techniques using BL21 (DE3), an *E. coli* bacterial expression system. rhBMP-2 was purified and refolded to active form, prior to use. rhBMP-2 (200 μg) was dissolved in a buffered solution and dropped onto the scaffold surface (*ca.* 1.5 cm^2). After solvent evaporation, C2C12 cells were seeded onto the scaffold surface as described above, and allowed to grow in culture medium. The alkaline phosphatase (ALP) activity of cells was tested after 4 days of culture. For this purpose, the culture medium was removed, the plate wells were washed with PBS (200 μL) and 100 μL/well of lysis buffer (50 mM Tris pH 6.8, 0.1% Triton X-100, 2 mM $MgCl_2$) was added. The resulting samples (10 μL) were assayed by using p-nitrophenylphosphate in 2-amino-2-methyl-1-propanol buffer as a substrate (total volume of 100 μL) at 37 °C for 10 min. Afterwards, the reaction was stopped with 100 μL of 0.5 M NaOH and the absorbance was measured at 450 nm on a Microplate Reader (Biotek FL-600).

Results and discussion

As mentioned above, the preparation of MWCNT/CHI scaffolds has been described in detail elsewhere.[19] Briefly, MWCNTs (6 wt. %) were dispersed in an aqueous solution of acetic acid (0.05 M, pH 5.5) also containing CHI (1 wt.%) (see Scheme in Fig. 1). CHI, a polysaccharide composed mainly of β-(1,4)-linked 2-deoxy-2-amino-D-glucopiroxane units, is the deacetylated product of chitin (poly *N*-acetyl-D-glucosamine, a well known natural biopolymer). Among other different polymers and surfactants, CHI has been found to be an efficient agent for CNT dispersion. This hybrid composition was very attractive for our purpose, given that it provided anionic Ca^{2+}-binding sites of great utility for mineralization purposes. The MWCNT/CHI suspension was frozen by unidirectional immersion into a liquid nitrogen bath. Subsequent freeze-drying resulted in self-supported monoliths mostly composed of MWCNTs (~85%), the cross-sectional view of which resembled a chamber-like architecture in the form of interconnected MWCNT/CHI sheets arranged in parallel layers crossed by pillars (Fig. 1a).

Among different strategies reported for mineralization,[25,26] we applied the urea assisted method (*i.e.* thermal treatment at 90 °C of an acid aqueous solution of HAp and urea which, at such a temperature, fully decomposes to carbon dioxide and ammonia) for scaffold mineralization.[22–24] Fig. 2 shows how the rise in pH (caused by ammonia coming from urea decomposition) resulted in a calcium and phosphorus concentration decrease in the solution as consequence of HAp precipitation. Complete precipitation occurred at *ca.* 4 hours for pH 6.5. Longer thermal treatments resulted in partial dissolution of precipitates and re-crystallization, as revealed the presence of a minor fraction of phosphorus in solution for reaction times above 4 hours. Nonetheless, the formation of carbonated HAp[27] was almost negligible even for reaction times of 12 hours (see FTIR spectrum in Fig. 3). TEM micrographs of HAp crystals obtained after mineralization for 4 and 12 hours revealed identical morphologies (*e.g.*, flower like crystals), the latter being larger than the former (3.75 versus 2.5 μm, respectively; see Fig. 4) most likely due to the above mentioned dissolution/re-crystallization processes.

In our case, the method followed for the mineralization of MWCNT/CHI scaffolds was analogous to that described above;

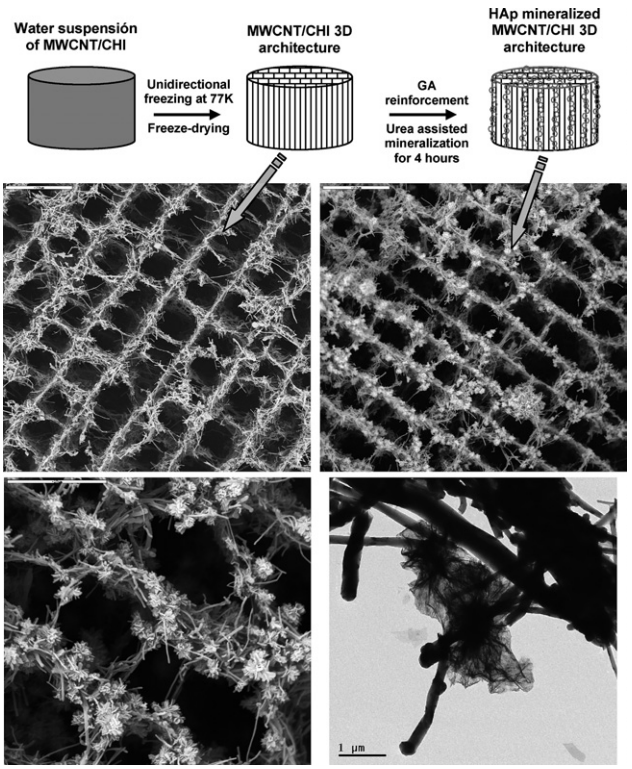

Fig. 1 Top row: Schematic representation of the cryogenic process followed for the preparation of MWCNT scaffolds and of the subsequent processes followed for GA architecture reinforcement and HAp mineralization (HAp crystals are represented as grease open circles). Middle row: SEM micrographs of MWCNT/CHI scaffolds (a) and HAp mineralized MWCNT/CHI scaffolds (b). Bars are 20 μm. Bottom row: SEM (c) and TEM (d) micrographs show a detail of HAp crystals on the MWCNT forming the scaffold. Bars are 10 and 1 μm, respectively.

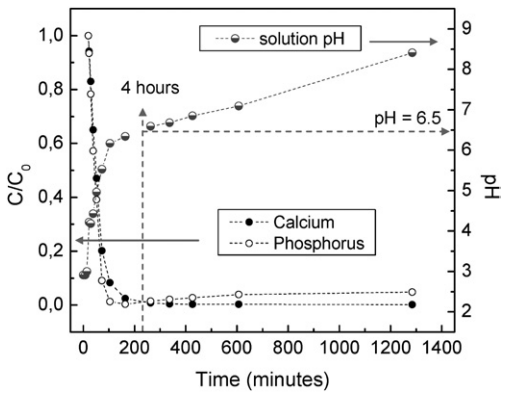

Fig. 2 Time evolution of calcium (solid circles) and phosphorus (open circles) relative concentration (left y axis), and pH (half-filled circles, right y axis) of the solution due to urea decomposition at 90 °C. Dashed arrows help for visualization of the Ca and P concentration and pH at 4 hours.

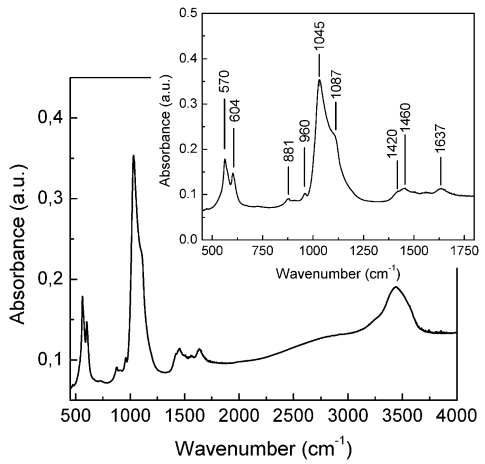

Fig. 3 FTIR spectrum of the precipitate resulting after 12 hours of urea decomposition. Phosphate groups in HAp show P–O stretching bands at *ca.* 1040 and 1090 cm^{-1} (υ_3) and bands at *ca.* 962–985 (υ_1) of lesser intensity. The υ_4 O–P–O bending mode appears in the range 570–630 cm^{-1}. The low intensity of the bands observed at 1420, 1460 and 880 cm^{-1} indicates traces of carbonates at the HAp crystals.

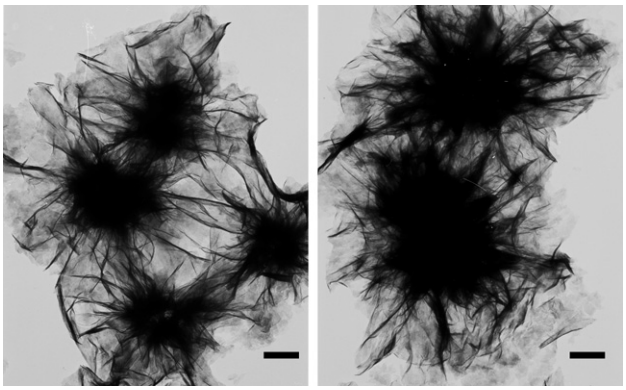

Fig. 4 TEM micrographs of HAp crystals resulting after mineralization for 4 (left) and 12 hours (right). Bars are 500 nm.

it was based on the immersion of the scaffolds in an acidic aqueous solution of HAp (15 mg/mL) containing urea (2 M) at room temperature, which, thereafter, was heat treated at 90 °C for 4 hours. Unfortunately, the MWCNT/CHI macrostructure collapsed under these conditions due to dissolution of CHI that interconnects the MWCNTs (not shown). Note that CHI exists as a cationic polyelectrolyte in acidic aqueous solutions and it is highly soluble. Actually, CHI only precipitates for pHs greater than 6. Thus, robustness improvement of the MWCNT/CHI macrostructure was required prior to mineralization. Reinforcement of the MWCNT/CHI architecture was achieved by cross-linking of the CHI linear chains with GA. The cross-linking chemistry of CHI with GA is well known and involves Schiff base formation.[28] Note that chemical modification of this polysaccharide polymer can be easily performed by covalent attachment of molecules to its amino and/or hydroxyl groups. The extent of the cross-linking can be easily controlled since it is proportional to the reaction time and the concentration of the cross-linker.[28] Thus, the MWCNT/CHI scaffold resulting after GA treatment was quite stable under the experimental conditions used for urea assisted mineralization (Fig. 1b). Note that the MWCNT scaffold structure exhibited some minor shrinkage (*ca.* 10%) after GA treatment (*i.e.* some reduction of the microchannels size can be observed in Fig. 1b as compared to Fig. 1a), most likely as a consequence of CHI cross-linking.

SEM micrographs of HAp mineralized MWCNT/CHI scaffolds (Fig. 1b and c) suggested the formation of discrete calcium phosphate clusters homogeneously adhered to the internal structure of the MWCNT/CHI 3D architecture. HAp crystal adhesion was ascribed to favorable electrostatic interactions between Ca^{2+} ions and CHI. The formation of spherical aggregates of *ca.* 1.0–1.2 μm built of plate like HAp crystals (shown in detail in Fig. 1c and d) is typical for crystalline apatite growth on bioactive glasses and polymer substrates (both natural and synthetic) using simulated body fluid mineralizations.[29] Interestingly, the HAp crystal size was significantly lower than for those obtained in solution, a typical feature of crystals mineralized on 2D and 3D supports.[13] The crystalline nature of the calcium phosphate clusters was corroborated by XRD; *i.e.* characteristic diffraction peaks matching those of crystalline apatites were assigned in Fig. 5). XRD also exhibited the main characteristic peaks for CNT at 26.5° and 54.3° (Fig. 5). Calibrated energy dispersion X-ray spectroscopy (EDS) analysis performed on the internal structure of HAp mineralized MWCNT/CHI scaffolds revealed a Ca/P ratio of 1.6 (in good agreement with that of HAp) throughout the monolith section (Fig. 6). This result confirmed the homogeneous distribution and the high affinity integration of the mineral into the 3D macrostructure. ICP-AES furthermore corroborated the above mentioned composition. The fractured samples did not lead to delamination of any mineral domains, suggesting good mineral–scaffold interfacial adhesion strength. Such a good interfacial adhesion (besides GA cross-linking) resulted in a significant improvement of robustness of the HAp mineralized MWCNT/CHI scaffolds (in terms of mechanical properties) as compared to the non-mineralized ones. Further details on this issue will be provided in a forthcoming paper.

Prolonged urea assisted mineralization processes (8 and 12 hours) resulted in a radial heterogeneous distribution of HAp crystals (see SEM of cross-sectioned MWCNT/CHI scaffolds in

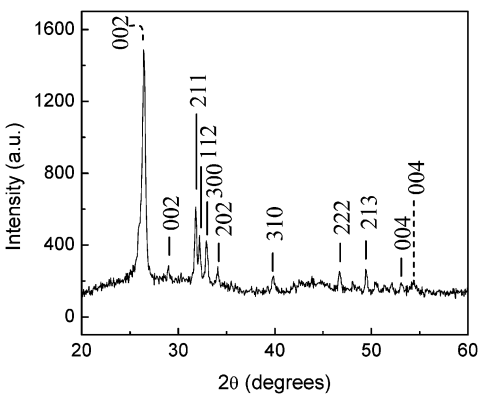

Fig. 5 XRD of HAp mineralized MWCNT/CHI scaffolds. Characteristic HAp and MWCNT diffraction peaks are marked with solid and dashed lines respectively.

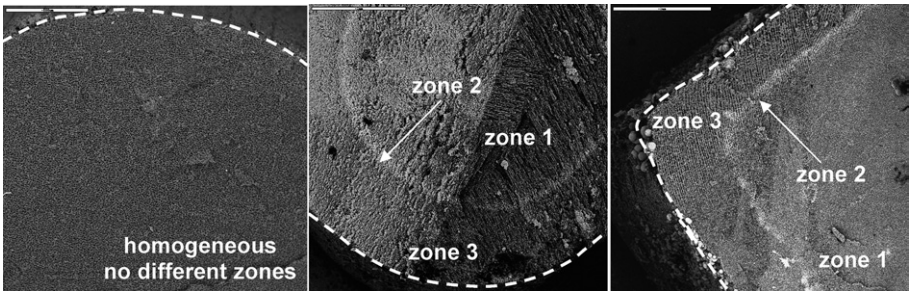

Fig. 6 Low magnification SEM micrographs of HAp mineralized MWCNT/CHI scaffolds with cylindrical (a, b) and cubic (c) shapes. White dashed lines indicate the perimeters of cylindrical and cubic monoliths. Urea assisted HAp mineralization was performed for 4 (a) and 12 (b, c) hours. Arrows indicate the bright monolith zone at which HAp concentrates. Bars are 500 μm for (a) and 1 mm for (b, c).

Fig. 6). Interestingly, the radial heterogeneity occurred no matter what the monolith shape (Fig. 6). This was corroborated by the appearance of a bright zone that, eventually, mimics the periphery of both cylindrical and cubic monoliths. A close inspection of cylindrical samples allowed the visualization of up to three zones with different HAp contents depending on the radial distance to the most inner zone of the monolith (Fig. 7a–c). The inner monolith (zone 1) exhibited an intermediate HAp content (Fig. 7a) that, eventually, increased at the bright zone (zone 2). Actually, zone 2 was the one with the greatest HAp content (Fig. 7d–e), with clusters of *ca.* 5 μm. Finally, HAp was depleted at the circle crown zone (zone 3) between the bright one and the outer side of the monolith (Fig. 7b). The occurrence of this radial HAp distribution should be ascribed to the calcium/phosphorus mass demanded by the large crystalline clusters (*ca.* 25 μm, Fig. 7c) growing at the external side of the monolith; *i.e.*

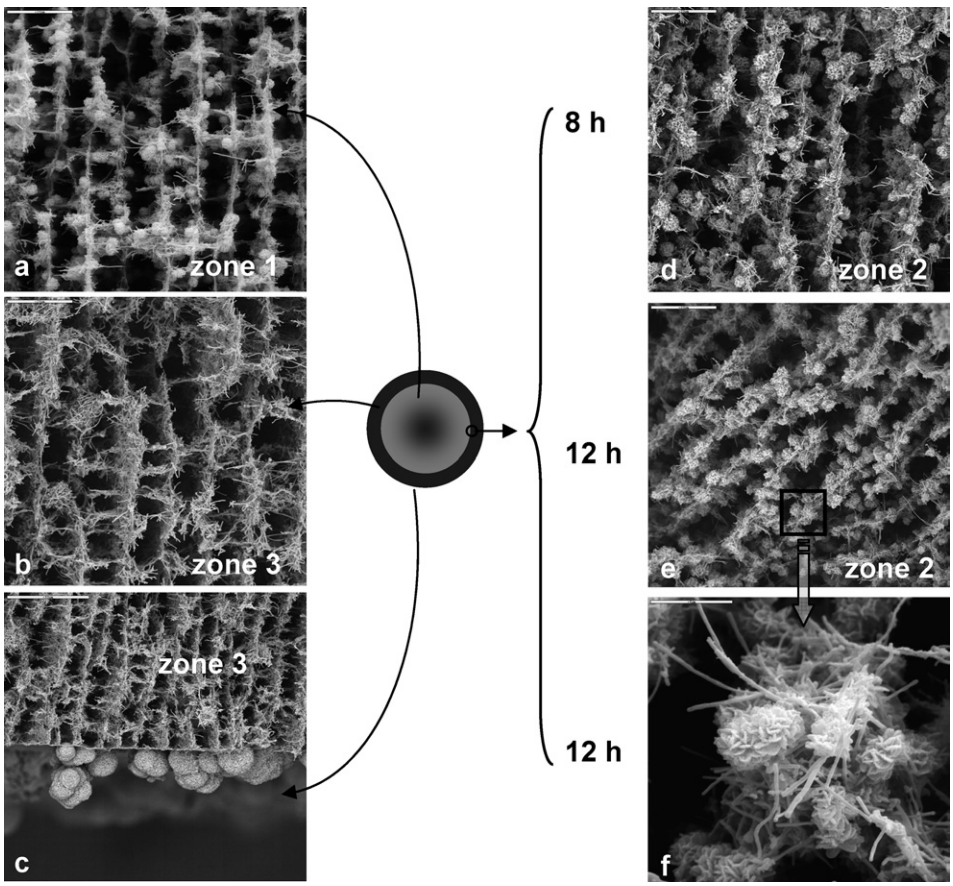

Fig. 7 Left column: SEM micrographs of cross-sectioned MWCNT/CHI scaffolds after HAp mineralization for 12 hours at different radial distances: (a) the inner zone ring, (b) the outer zone ring and (c) the outer monolith side. Bars are 20 μm for (a) and (b) and 50 μm for (c). Middle column: Schematic representation of the cross-sectioned HAp gradient concentration formed upon prolonged mineralization of the MWCNT/CHI scaffold. Right column: SEM micrographs of cross-sectioned MWCNT/CHI scaffolds after HAp mineralization for 8 (d) and 12 (e) hours, at the radial distance of maximum HAp concentration. Bars are 20 μm. SEM micrograph (f) shows a detail of the HAp crystalline cluster growth at the ring zone. Bar is 5 μm.

ART ■ B815401E

in a typical Ostwald ripening process, large crystals grow at the expense of the smaller crystals by dissolution and re-crystallization. However, Ca and P consumption by these large crystals was eventually faster than Ca and P diffusion through the scaffold macrostructure which, ultimately, caused Ca and P depletion at the periphery of the monolithic macrostructure (zone 3). Disruption of the homogeneous HAp gradient across the monolith determined the formation of a crown of HAp crystalline clusters of *ca.* 5 μm at zone 2 (Fig. 7f). These crystalline clusters were smaller than those formed outside the scaffold (due to the above mentioned template effect of the MWCNT macrostructure on the crystals growth), but larger than those of *ca.* 1.2 μm (Fig. 1c,d) originally mineralized after 4 hours (due to the above mentioned Ostwald ripening process).

The occurrence of crystal dissolution and re-crystallization within the HAp mineralized MWCNT/CHI scaffold could be of interest for bone tissue engineering purposes (as mentioned in the introduction, it determines the scaffold suitability for *in vivo* applications). However, the design of a procedure for homogeneous scaffold mineralization was also highly desired. For this purpose, we performed a second attempt of mineralization following a slightly different procedure (*e.g.*, route (b) described in the experimental part), i.e. the thermal treatment of the soaked scaffold out of rather than in the soaking solution. Thus, homogeneously distributed HAp crystals precipitated throughout the whole 3D scaffold structure (no matter whether mineralization is prolonged for 4 or 12 hours), due to the avoided precipitation of HAp crystals outside the scaffold structure. The HAp crystals were also flower like and *ca.* 1 μm in diameter (Fig. 8), in the same range as those obtained by procedure (a) for short reaction times (*e.g.*, 4 hours). Actually, XRD and FTIR spectrum of this sample are analogues to those shown in Figs. 3 and 5. The flower like crystals shown in Fig. 8 were analyzed by SAED (Fig. 9). The obtained spotty ring SAED pattern was characteristic of polycrystalline HAp crystals, in particular, of agglomerated thin platelets elongated in the c direction.[30] As a rule, the characteristic HAp spacing of 0.816 nm between (110) planes is not seen in polycrystalline electron diffraction patterns due to the high background intensity close to the central spot. Thus, the closest spot (to the central one) on this SAED pattern belonged to the (101) planes with $d_{101} = 0.530$ nm. Some other strong reflections belonging to (002), (210), (211), (202), (310), (222) and (213) planes could also be observed with $d_{002} = 0.347$ nm, $d_{210} = 0.319$ nm, $d_{211} = 0.284$ nm, $d_{202} = 0.262$ nm, $d_{310} = 0.228$ nm, $d_{222} = 0.194$ nm and $d_{213} = 0.185$ nm (Fig. 9). ICP-AES and EDS analysis also revealed a Ca/P ratio of 1.6, characteristic of HAp.

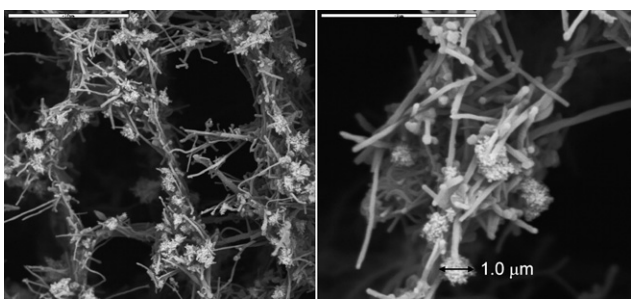

Fig. 8 SEM micrographs of cross-sectioned MWCNT/CHI scaffolds after Hap mineralization for 4 hours following procedure (b). Bars are (left) 10 μm and (right) 5 μm.

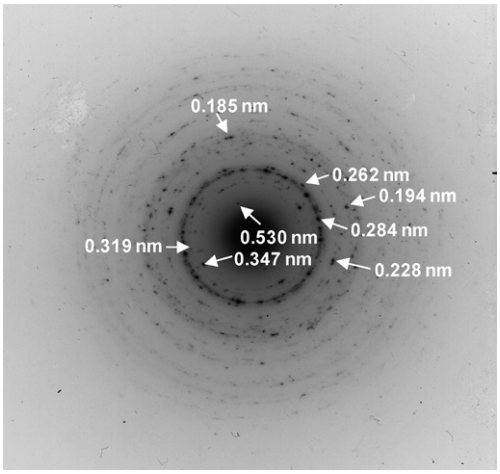

Fig. 9 SAED pattern of agglomerated flower like polycrystalline HAp formed by elongated platelet crystals and entrapped within the three-dimensional architecture of MWCNT/CHI scaffolds.

Given the above mentioned controversy about CNT cytotoxicity, we decided to study the proliferation and viability of pre-osteoblastic C2C12 cells on HAp mineralized MWCNT/CHI scaffolds. Environmental scanning electron microscopy (ESEM) measurements permitted the visualization of cells with *ca.* 10–20 μm diameter (inset of Fig. 10) uniformly spread onto the surface of scaffolds cultured for 4 days (Fig. 10). This result was a clear indication of the efficient cell growth and proliferation on the scaffold surface. In spite of the fact that most of the surface of the HAp mineralized MWCNT/CHI scaffold was hidden beneath such a confluent layer of cells, preservation (at least, partial) of the scaffold patterned structure could still be distinguished, independent of the scaffold hydration in the cell culture medium. The scaffold biocompatibility was further corroborated by measurements of the metabolic conversion of 3-(4,5-dimethylthiazol-2-yl)-2,5-diphenyltetrazoliumbromide (MTT). This assay is based on the ability of cell mitochondria to reduce MTT into a formazan precipitate that can be dissolved in *n*-propanol. The spectrophotometric quantification of the n-propanol

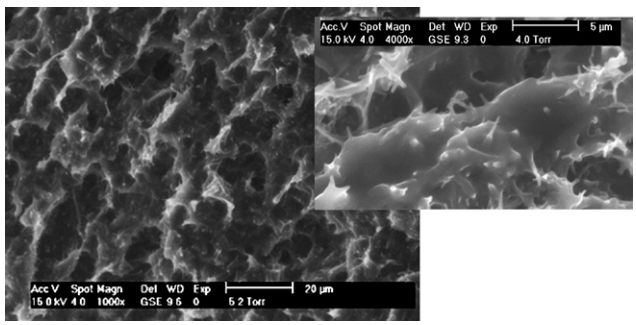

Fig. 10 ESEM micrographs of HAp mineralized MWCNT/CHI scaffolds seeded with C2C12 cells and cultured for 4 days (bar is 20 μm.). Inset shows a detail of cultured cells adhered on HAp mineralized MWCNT/CHI scaffolds (bar is 5 μm).

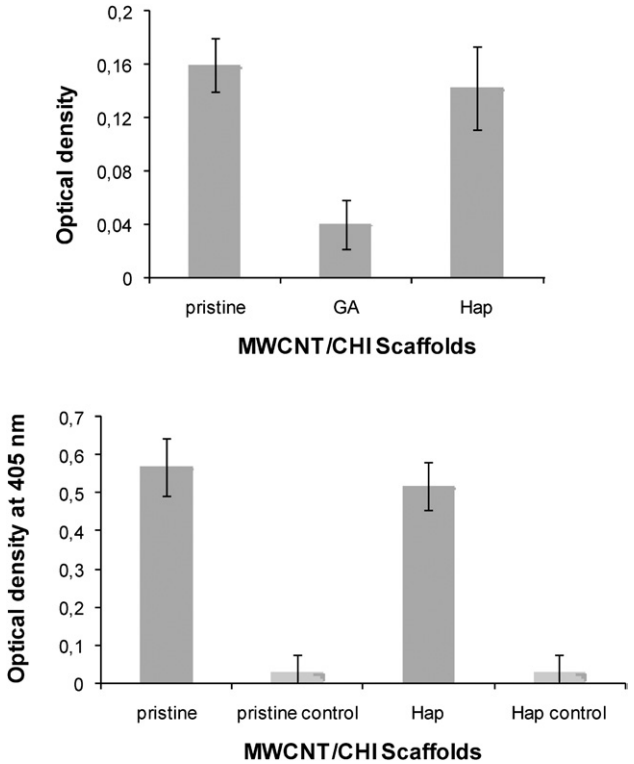

Fig. 11 Top: MTT cytotoxicity assays for C2C12 cell seeded on the surface of MWCNT/CHI scaffolds (pristine, GA treated and HAp mineralized after GA treatment) and growth for four days. Bottom: ALP activity of C2C12 cell growth for four days on the surface of MWCNT/CHI scaffolds (pristine and HAp mineralized after GA treatment) impregnated or not (negative controls) with rhBMP-2.

solution of formazan allowed us to monitor the vitality and biochemical activity of cells seeded onto the patterned surface of HAp mineralized MWCNT/CHI scaffolds. Interestingly, the biocompatibility found for the mineralized scaffolds was in the same range as that observed in our previous work for plain MWCNT/CHI scaffolds (Fig. 11).[19c] Note that some partial lack of biocompatibility due to the use of GA as cross-linking agent was recovered after HAp mineralization. GA could indeed be replaced by some other more biocompatible cross-linking agents (*e.g.*, genipin),[31] but, in our case, its use was quite helpful to emphasize the scaffold biocompatibility enhancement resulting after HAp mineralization.

Moreover, the ability of adsorbed C2C12 cells to differentiate towards collagen expressing cells in the presence of the recombinant human protein BMP-2 (rhBMP-2)[32] would make HAp mineralized MWCNT/CHI scaffolds quite promising for bone tissue growth. It is important to highlight that one must attempt to mimic tissue properties (in terms of both structure and composition) to really recover proper function and organization of native tissues. For this purpose and taking advantage of the affinity exhibited by different proteins to be adsorbed on CNT (and in particular, for MWCNT),[33–35] we adsorbed rhBMP-2 (a protein that is a potent osseoinductor) on both MWCNT/CHI and HAp mineralized MWCNT/CHI scaffolds (see experimental for details). The preservation of rhBMP-2 activity after adsorption and, hence, its capability to differentiate C2C12 cells towards the osteoblastic lineage was evaluated following the emergence of ALP activity (an early osteogenic marker related to matrix mineralization processes and absent in C2C12 cell line).[32] The ALP activity reached by cells adhered on mineralized scaffolds was in the range that we have recently reported for non-mineralized scaffolds (Fig. 11).[19c] This feature confirmed the occurrence of differentiation of C2C12 cells adhered on HAp mineralized MWCNT/CHI scaffolds. Negligible ALP activity (Fig. 11) was obtained for both mineralized and non-mineralized scaffolds without rhBMP-2 (*i.e.*, negative controls).

Conclusions

In summary, we have applied the ISISA process for the preparation of MWCNT/CHI scaffolds, the chemical composition and macrostructure of which make them quite suitable for mineralization purposes. Short mineralization times (*e.g.*, 4 hours) are recommended for the achievement of HAp crystalline clusters homogeneously distributed throughout the scaffold macrostructure. Mineralization for extended periods of time may result (depending on the mineralization procedure) in crystal dissolution, mass diffusion throughout the monolith structure and re-crystallization and, as a consequence, in the formation of crystalline clusters of larger size than the original ones (5 μm versus 1 μm, respectively). Moreover, we have demonstrated the *in vitro* suitability of HAp mineralized MWCNT/CHI scaffolds for proliferation and viability of C2C12 cells which have also been able to differentiate towards osteoblastic lineage in the presence of rhBMP-2. Besides the above mentioned occurrence of HAp crystal dissolution and re-crystallization across the scaffold structure, the capability to mimic both bone structure (trabecular type) and composition (HAp and collagen) should make HAp mineralized MWCNT/CHI scaffolds quite promising for bone tissue engineering purposes.

Acknowledgements

This work was supported by S-0505/PPQ-0316, MAT2006-02495, 200660F01 and 200760I009 Projects. We also acknowledge TPA Inc. for financial support. M. C. G. acknowledges CSIC for an I3P research contract.

References

1 H. Cölfen and S. Mann, *Angew. Chem. Int. Ed.*, 2003, **42**, 2350–2365.
2 K. J. C. van Bommel, A. Friggeri and S. Shinkai, *Angew. Chem. Int. Ed.*, 2003, **42**, 980–999.
3 K. Naka and Y. Chujo, *Chem. Mater.*, 2001, **13**, 3245–3259.
4 T. J. Webster, C. Ergun, R. H. Doremus, R. W. Siegel and R. Bizios, *Biomaterials*, 2001, **22**, 1803–10.
5 Y.-F. Chou, W.-A. Chiou, Y. Xu, J. C. Y. Dunn and B. M. Wu, *Biomaterials*, 2004, **25**, 5323–5331.
6 Zoe A. C. Schnepp, R. Gonzalez-McQuire and S. Mann, *Adv. Mater.*, 2006, **18**, 1869–1872.
7 H.-W. Kim, J.-H. Song and H.-E. Kim, *Adv. Funct. Mater.*, 2005, **15**, 1988.
8 H. Ehrlich, T. Douglas, D. Scharnweber, T. Hanke, R. Born, S. Bierbaum and H. Worch, *Z. Anorg. Allg. Chem.*, 2005, **631**, 1825–1830.
9 V. M. Rusu, C. Ng, M. Wilke, B. Tiersch, P. Fratzi and M. G. Peter, *Biomaterials*, 2005, **26**, 5414–5426.
10 W. L. Murphy and D. J. Mooney, *J. Am. Chem. Soc.*, 2002, **124**, 1910.

11 D. Enlow, A. Rawal, M. Kanapathipillai, K. Schmidt-Rohr, S. Mallapragada, C.-T. Lo, P. Thiyagarajan and M. Akinc, *J. Mater. Chem*, 2007, **17**, 1570–1578.
12 S.-H. Yu, H. Cölfen and M. Antonietti, *J. Phys. Chem. B*, 2003, **107**, 7396–7405.
13 J. Song, V. Malathong and C. R. Bertozzi, *J. Am. Chem. Soc.*, 2005, **127**, 3366–3372.
14 S. Elhadj, E. A. Salter, A. Wierzbicki, J. J. De Yoreo, N. Han and P. M. Dove, *Crystal Growth & Design*, 2006, **6**, 197–201.
15 L. Wang, S. R. Qiu, W. Zachowicz, X. Guan, J. J. DeYoreo, G. H. Nancollas and J. R. Hoyer, *Langmuir*, 2006, **22**, 7279–7285.
16 H. Yan, K. Zhang, C. F. Blanford, L. F. Francis and A. Stein, *Chem. Mater*, 2001, **13**, 1374–1382.
17 S. Aryal, K. C. R. Bahadur, N. Dharmaraj, K.-W. Kim and H. Y. Kim, *Scripta Mater.*, 2006, **54**, 131–135.
18 B. Zhao, H. Hu, S. K. Mandal and R. C. Haddon, *Chem. Mater.*, 2005, **17**, 3235–3241.
19 (*a*) M. C. Gutierrez, M. J. Hortigüela, R. Jiménez, J. M. Amarilla, M. L. Ferrer and F. del Monte, *J. Phys. Chem. C*, 2007, **111**, 5557; (*b*) M. C. Gutierrez, Z. Y. Garcia-Carvajal, M. J. Hortigüela, L. Yuste, F. Rojo, M. L. Ferrer and F. del Monte, *J. Mater. Chem.*, 2007, **17**, 2992; (*c*) A. Abarrategui, M. C. Gutierrez, M. J. Hortigüela, V. Ramos, J. L. Lopez-Lacomba, M. L. Ferrer and F. del Monte, *Biomaterials*, 2008, **29**, 94.
20 (*a*) Among others: S. R. Mukai, H. Nishihara and H. Tamon, *Chem. Commun.*, 2004, 874; (*b*) H. Nishihara, S. R. Mukai and H. Tamon, *Carbon*, 2004, **42**, 889; (*c*) Zhang, I. Hussain, M. Brust, M. F. Butler, S. P. Rannard and A. I. Cooper, *Nat. Mater.*, 2005, **4**, 787; (*d*) S. Deville, E. Saiz, R. K. Nalla and A. P. Tomsia, *Science*, 2006, **311**, 515; (*e*) S. Bandi and D. A. Schiraldi, *Macromolecules*, 2006, **39**, 6537–6545.
21 (*a*) M. C. Gutierrez, M. Jobbagy, N. Rapun, M. L. Ferrer and F. del Monte, *Adv. Mater.*, 2006, **18**, 1137; (*b*) M. L. Ferrer, R. Esquembre, I. Ortega, C. R. Mateo and F. del Monte, *Chem. Mater.*, 2006, **18**, 554; (*c*) M. C. Gutierrez, Z. Y. Garcia-Carvajal, M. Jobbagy, F. Catalina, C. Abrusci, L. Yuste, F. Rojo, M. L. Ferrer and F. del Monte, *Chem. Mater.*, 2007, **19**, 1968; (*d*) M. C. Gutierrez, Z. Y. Garcia-Carvajal, M. Jobbagy, L. Yuste, F. Rojo, M. L. Ferrer and F. del Monte, *Adv. Funct. Mater.*, 2007, **17**, 3505–3513; (*e*) M. C. Gutierrez, M. Jobbagy, M. L. Ferrer and F. del Monte, *Chem. Mater.*, 2007, **20**, 11–13; (*f*) for a recent review see: M. C. Gutierrez, M. L. Ferrer and F. del Monte, *Chem. Mater.*, 2007, **20**, 634–648.
22 J. Zhan, Y.-H. Tseng, J. C. C. Chan and C.-Y. Mou, *Adv. Funct. Mater.*, 2005, **15**, 2005–2010.
23 J. Zhan, H.-P. Lin and C.-Y. Mou, *Adv. Mater.*, 2003, **15**, 621–623.
24 Jie. Song, E. Saiz and C. R. Bertozzi, *J. Am. Chem. Soc.*, 2003, **125**, 1236–1243.
25 T. Wang, M. Antonietti and H. Cölfen, *Chem. Eur. J.*, 2006, **12**, 5722–5730.
26 A.-W. Xu, Y. Ma and H. Cölfen, *J. Mater. Chem.*, 2007, **17**, 415–449.
27 H. Morgan, R. M. Wilson, J. C. Elliott, S. E. P. Dowker and P. Anderson, *Biomaterials*, 2000, **21**, 617–627.
28 M. Zhang, A. Smith and W. Gorski, *Anal. Chem.*, 2004, **76**, 5045–5050.
29 T. Kokubo, H.-M. Kim and M. Kawashita, *Biomaterials*, 2003, **24**, 2161–2175.
30 E. I. Suvorova and P. A. Buffat, *J. Micros.*, 1999, **196**, 46–58.
31 F.-L. Mi, Y.-C. Tan, H.-F. Liang and H.-W. Sung, *Biomaterials*, 2002, **23**, 181–191.
32 T. Katagiri, A. Yamaguchi, M. Komaki, E. Abe, N. Takahashi, T. Ikeda, V. Rosen, J. M. Wozney, A. Fujisawa-Sehara and T. Suda, *J. Cell. Biol.*, 1994, **127**, 1755–66.
33 H. Hu, Y. Ni, V. Montana, R. C. Haddon and V. Parpura, *Nano Lett.*, 2004, **4**, 507–11.
34 B. R. Azamian, J. J. Davis, K. S. Coleman, C. B. Bagshaw and M. L. H. Green, *J. Am. Chem. Soc.*, 2002, **124**, 12664–65.
35 H. M. So, K. Won, Y. H. Kim, B. K. Kim, B. H. Ryu, P. S. Na, H. Kim and J. O. Lee, *J. Am. Chem. Soc.*, 2005, **127**, 11906–7.

ART ■ B815401E

Authors Queries

Journal: **JM**

Paper: **b815401e**

Title: **Urea assisted hydroxyapatite mineralization on MWCNT/CHI scaffolds**

Editor's queries are marked like this... **1**, and for your convenience line numbers are inserted like this... 5

Query Reference	Query	Remarks
1	For your information: You can cite this article before you receive notification of the page numbers by using the following format: (authors), J. Mater. Chem., 2008, DOI: 10.1039/b815401e.	
2	The mentions of coloured bars have been removed from Fig. 11 caption and the main text, since the figure is to be reproduced in black and white.	